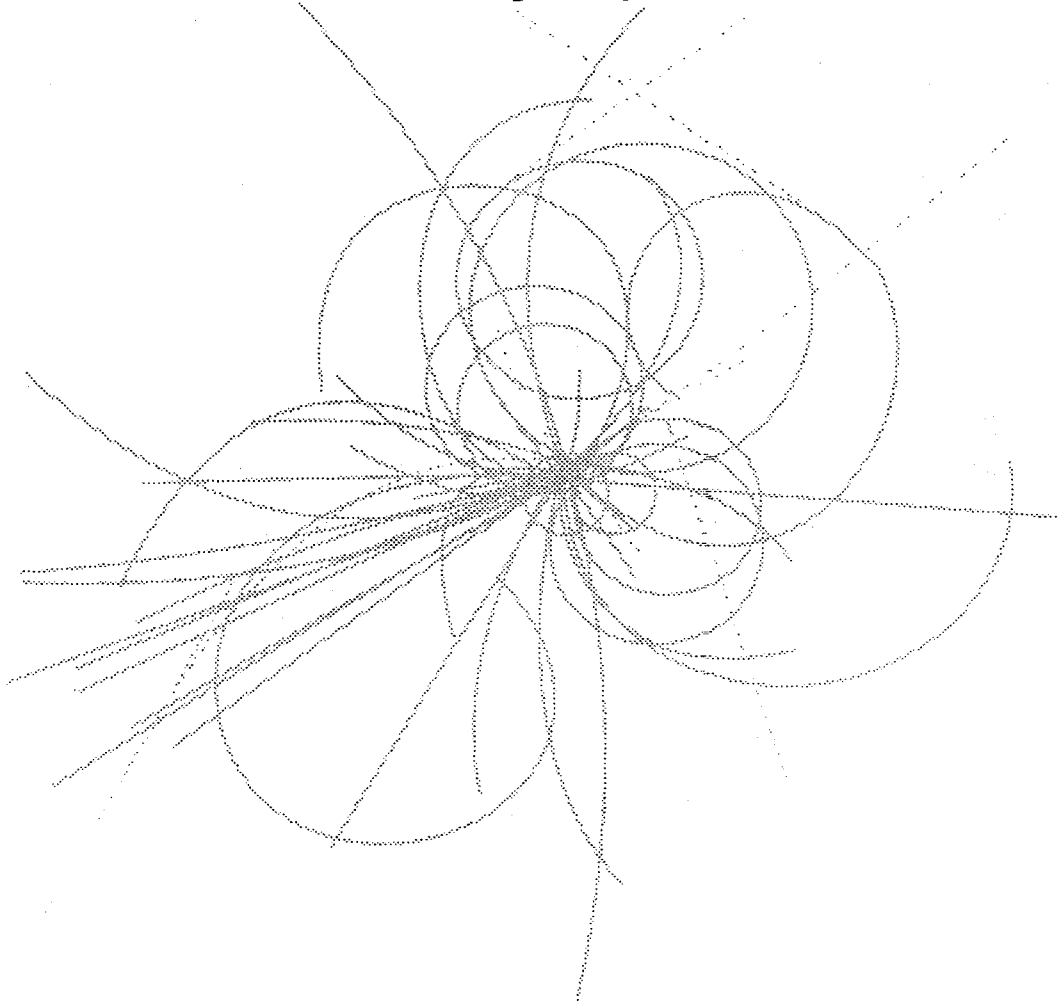


Superconducting Super Collider Laboratory



Design Characteristics of the Linac— LEB Transfer Line for the SSC

R. Bhandari, E. Seppi, and S. Penner

May 1991

**Design Characteristics of the Linac—
LEB Transfer Line for the SSC***

R. Bhandari, E. Seppi, and S. Penner

Superconducting Super Collider Laboratory[†]
2550 Beckleymeade Ave.
Dallas, TX 75237

May 1991

*Presented at the 1991 IEEE Particle Accelerator Conference, San Francisco, CA, May 6–9, 1991.

[†]Operated by the Universities Research Association, Inc., for the U.S. Department of Energy under Contract No. DE-AC02-89ER40486.

Design Characteristics of the Linac - LEB Transfer Line for the SSC

R. K. Bhandari, E. Seppi and S. Penner
Superconducting Super Collider Laboratory*, Dallas, Texas 75237, USA

Abstract

This paper describes an H^- beam transfer line from the 600 MeV Coupled Cavity Linac to the Low Energy Booster synchrotron of the SSC injector complex. The design takes into consideration space charge effects, the need for beam diagnostics, the effects of magnetic field imperfections, radiation safety and future upgrade possibilities.

I. INTRODUCTION

A properly matched, stable and clean H^- beam of small momentum spread and emittance is to be delivered to the stripper foil in the LEB. Beam simulations studies show that the transverse emittance at the linac exit is approximately 0.2π mm-mrad (rms, normalized) in each plane and the longitudinal emittance is about 216π keV-deg.(rms) at the CCL operational frequency of 1284 MHz. The nominal average beam current in the linac macropulse is 25 mA with pulse lengths of 6.6 μ s for collider ring filling and up to 35 μ s for test beam operations. Our first design of the transfer line [1] consisted of a FODO transport line, emittance scraper section, an achromatic spectrometer, emittance measurement section, phase space matching section and injection section. As a result of a new requirement of controlling the dispersion (η and η') at the exit of the last injection bump magnet, a dispersion matching section has been incorporated between the phase space matching section and the septum magnet. Further, in order to meet the "failsafe" radiation safety requirements, the beam now goes to a dump when the second dipole of the achromatic spectrometer is off. (In the first design, an additional dipole magnet was used to divert the beam to the dump). Other segments of the transfer line have also been reconfigured or modified as a result of these requirements and for improved performance. Computer codes TRANSPORT, TRACE-3D and TURTLE were used for these calculations.

II. DESCRIPTION OF THE TRANSFER LINE

Figure 1 shows the layout of the transfer line. A 98 m long straight section beyond the linac exit has been provided for a future upgrade of the linac energy to 1 GeV. The first 10.3 m of this section is a four-quadrupole matching system to prepare the input beam for the FODO array. This array consists of 10 cells of 90 degrees phase advance each, to transport the beam over the remaining 87.7 m. Quadrupoles in this section have 30 mm aperture diameter while those on the rest of the line have an aperture diameter of 75-100 mm.

Two quadrupole doublets Q1,Q2 and Q3,Q4 in the 38 m long section between the FODO array and the achromatic spectrometer permit emittance measurement of the beam when it is being transported to either of the beam dumps. This allows linac tuneup without generating radiation in the LEB area. Three wire scanners, downstream of Q2, are used to measure the transverse emittance in this section. The last two quadrupoles of the FODO array and Q1,Q2 are adjusted to produce a double waist at the central wire scanner at 'A'. The betatron phase advance between successive scanners is approximately 60 degrees in both planes. This configuration is optimum for emittance reconstruction [2]. In the tuneup mode, the first dipole magnet (D1) of the spectrometer is turned off and doublet Q3,Q4 transports the beam to dump 1. In the injection mode, the abovementioned six quadrupoles are used to tune the beam for further transport to the LEB. Major constraints in this case are a double waist with a small and controllable x-waist size for good resolution at the center of the achromat, 'B', small vertical beam size in the dipole gaps and an x-waist at 'A'. The last condition is needed for accurate energy spread measurement.

Transverse emittance scraping to remove extreme tails from the beam will be done in this section using two stripper scrapers. The first scraper is placed near the location 'A' and the second near the entrance of Q3 after a 90 degrees of phase advance. The scraped negative ions are mostly converted into

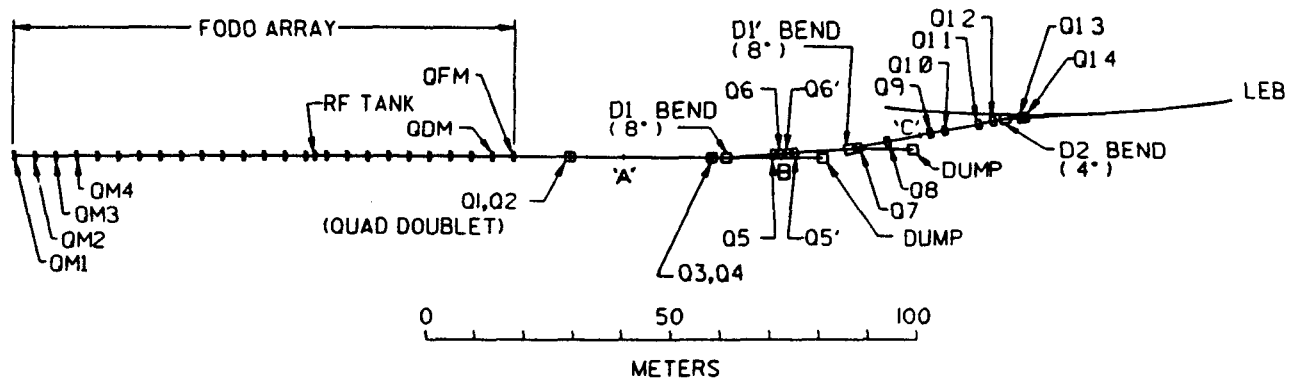


Figure 1: Layout of the beam transfer line between the coupled cavity linac and the low energy booster synchrotron for the SSC. Q: Quadrupole magnets, and D: Dipole magnets. Total length of the transfer line is about 205 meters.

*Operated by the Universities Research Association, Inc. for the U.S. Department of Energy under Contract No. DE-AC02-89ER40486.

positive ions and bent in the opposite direction by D1. TURTLE calculations show that most of these ions can be transported to the dump.

Each of the dipoles of the symmetric achromatic spectrometer bends the beam by 8.0 degrees. The effective length of the dipoles is 2 m, which is determined by the need to limit the magnetic field to 0.4 T to bend 1 GeV H^- beam with negligible stripping losses [3]. Dispersion (η) at the center of the achromat is 2.05 m. For a monoenergetic x-waist size ($2\sigma_x$) of 0.6 mm at this point, the momentum resolution is 0.03% (rms). This x-waist is an image of the x-waist at location 'A' and the magnification is about 0.8. This relationship is used to determine the energy spread from beam profile measurements at the wire scanner at 'B'. Two sextupole magnets, one each at the entrance and exit of the achromat section, are provided to correct for the second order field inhomogeneity effects in the dipoles (sec. V)

Downstream of the spectrometer, in another straight section, precise determination of the transverse emittance will be carried out in the same manner as at the upstream location. Quadrupoles Q7 and Q8 make the beam almost circular and form a double waist at the central wire scanner at location 'C'. Distance between the successive wire scanners is about 2 m.

The transverse phase space matching system for the injection process consists of four quadrupoles Q9 to Q12. It is located in a dispersion free region and has been configured to match a wide range of α and β values at the stripper.

The dispersion matching system consists of a 4.0 degree dipole magnet (D2) and two quadrupoles Q13 and Q14. Its function is to obtain vanishing η and η' at the exit of the fourth bump magnet, where the injected beam coincides with the LEB central orbit. D2 is 1 m long and bends the beam in the same direction as the septum magnet. Parameters of this system have been optimized such that for the dynamic range of transverse phase space matching, beam envelopes and field gradients remain within reasonable limits. During operation, tuning of the dispersion matching system will be done before the tuning of the transverse phase space matching system.

A septum magnet and four bump magnets constitute the injection system. The septum magnet, excited by a 3 ms half-sine wave current waveform, guides the beam into the second bump magnet. All four bump magnets are energized by one power supply providing a trapezoidal waveform with rise, fall and flattop times of 40 μ s.

III. ENERGY COMPRESSOR

The energy compressor is a 1.85 m long RF tank similar to the last coupled cavity tank of the linac. It consists of 20

cells and operates at a synchronous phase of -90 degrees and thus provides no acceleration for the central particle. Its function is to control the energy spread at the stripper for efficient RF capture by the LEB. The tank has been placed at 59.8 m downstream of the linac exit in the 6th cell of the FODO array. At this location the rms bunch length for 25 mA average beam current is 23.3 degrees. TRACE-3D calculations show that the rms energy spread grows from 168 keV to 600 keV from the linac exit to compressor entrance. The desired energy spread of 100 keV at the stripper, about 145 m downstream, can be achieved with an average accelerating gradient (E_0T) of 0.8 MV/m. The resulting rms bunch length is 29.5 degrees. The rms energy spread at the center of the achromat for these settings is 69 keV.

IV. SPACE CHARGE EFFECTS

Space charge effects have been evaluated using TRACE-3D, which employs a linear approximation for the charge density. The quadrupole settings need significant readjustments to preserve the optical modes of beam transport described in sec. II. Optimization for these effects is carried out in several steps. In step 1, the matching quadrupoles, QM1-QM4, at the linac exit are varied to obtain matched α and β values for the FODO array. Quadrupoles of the array are left at their zero beam current values. In step 2, the last two quadrupoles of the FODO array, QDM and QFM, are adjusted to obtain an x-waist, the same as for the zero beam current case, at location 'A'. Step 3 involves producing a double waist at the location 'B' by tuning the quadrupoles Q3 and Q4. Step 4 requires adjustment of Q5,5'(coupled) and Q6,6'(coupled) to make η and η' zero at the exit of the achromatic spectrometer. Prior to this step, $\eta=0.68$ m and $\eta'=0.05$ for 25 mA beam current when tuned to zero for a zero current beam. Since, as a result of optimization, the field strengths of these quadrupoles change from their zero beam current values, the beam centroid is not transported in an exactly achromatic manner. Its displacement from the optic axis due this effect is ~ 1 mm/percent momentum error, which is negligible. Step 5 involves forming a double waist at the location 'C' by tuning Q7 and Q8. Step 6 involves obtaining $\eta=\eta'=0$ at the exit of fourth bump magnet by adjusting Q13 and Q14. Finally, in step 7 quadrupoles Q9 to Q12 are tuned to obtain the desired transverse phase space matching at the stripper. Steps 6 and 7 may have to be iterated a few times to obtain the desired tolerances on the matrix elements' values. Tuning of E_0T of the energy compressor may be necessary, which may require iteration of steps 2 to 7. Figure 2 shows the beam envelopes in the transfer line optimized for 25 mA beam current.

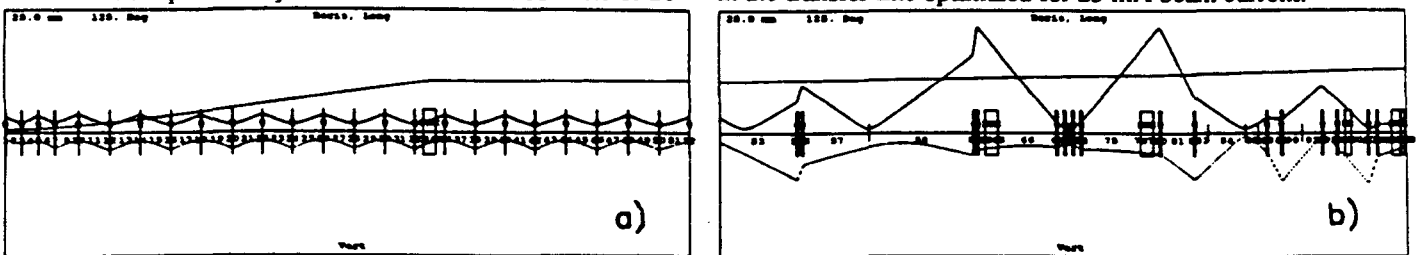


Figure 2: Envelopes for 90% beam in the transfer line optimized for 25 mA beam current. These plots were obtained using TRACE-3D for (a) the FODO array, and (b) rest of the transfer line up to the stripper in the LEB ring. E_0T for the energy compressor cavity is set at 0.8 MV/m.

Table 1 compares the quadrupole settings for zero beam current and the optimized 25 mA beam current cases. Transverse and longitudinal emittances at the linac exit are ~2 times larger for 50 mA beam current. Space charge optimization for this beam shows that the changes, relative to 25 mA settings, are within $\pm 5\%$ for most of the quadrupoles.

TABLE 1

Step #	Quad name	Pole tip field (kG) for		Change (kG)
		No beam Current	25 mA beam Current	
1	QM1	3.6798	3.8596	+0.1798
	QM2	-2.9026	-3.8498	+0.9472
	QM3	2.4871	3.5220	+1.0349
	QM4	-3.2876	-3.6995	+0.4119
2	QDM	-2.8985	-2.5694	-0.3291
	QFM	3.3998	3.5276	+0.1278
3	Q3	-2.4453	-2.6761	+0.2308
	Q4	2.5499	2.6978	+0.1479
4	Q5,5'	-1.2130	-1.2224	+0.0094
	Q6,6'	1.2130	1.2649	+0.0519
5	Q7	1.0056	1.0084	+0.0028
	Q8	-1.1560	-1.1678	+0.0118
6	Q13	-2.8241	-2.7217	-0.1024
	Q14	3.5579	3.4967	-0.0612
7	Q9	2.1643	1.7534	-0.4109
	Q10	-2.1667	-2.1472	-0.0195
	Q11	0.2342	1.2288	+0.9946
	Q12	1.2612	0.0905	-1.1707

V. MAGNETIC FIELD AND POSITION ERRORS

Estimation of the effects of magnetic field errors on the beam has been carried out using TURTLE. Histograms for the horizontal and vertical phase spaces were obtained. Figure 3 shows x-x' histograms at the center of the achromatic spectrometer in different cases. It is seen that severe distortion occurs even for a moderate second order field variation (sextupole component) of 5×10^{-4} at 1 cm from the central ray in dipole D1. This would result in significant loss of beam at the scraper. Weak sextupole magnets will be used to correct this error (figure 3). Effects of higher multipole components

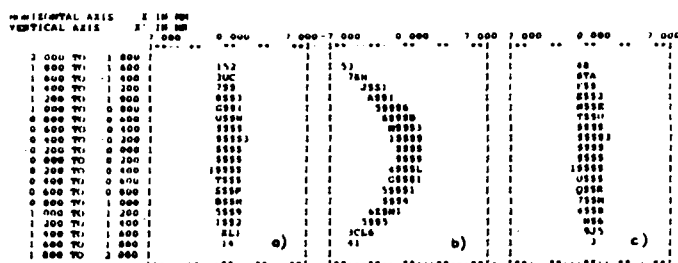


Figure 3: x-x' histograms at the center of the achromat with (a) no sextupole component in D1, (b) 0.05% sextupole component in D1 and (c) its compensation using a sextupole magnet with B''L of 2.03 T/m placed 0.5 m upstream of D1.

in the quadrupole fields were estimated by comparing the resulting distorted histograms at the stripper with the ideal histograms. Over 99% of the rays fall within the boundary of the ideal histograms if the pole tip fields due to sextupole, octupole, decapole and duodecapole components remain below 1.0%, 0.2%, 1.0% and 0.5%, respectively, of the quadrupole pole tip field in the larger magnets. Tolerances for the smaller quadrupoles on the FODO array are several times larger.

Effects of magnet position errors were estimated using TRANSPORT. Studies were primarily concentrated on emittance growth due to rotation of the quadrupoles about the optic axis. A minor modification of TRANSPORT allows the application of up to 250 sets of random errors to the transfer line magnets in a single run. Figure 4 shows the results of calculations for two cases of rotation errors. It is noticed that the emittance enlargement can be appreciably reduced by applying stricter alignment accuracy on the quadrupoles Q1, Q2, Q3 and Q4. FODO quadrupoles are much less sensitive to the alignment errors than the larger quadrupoles of the transfer line.

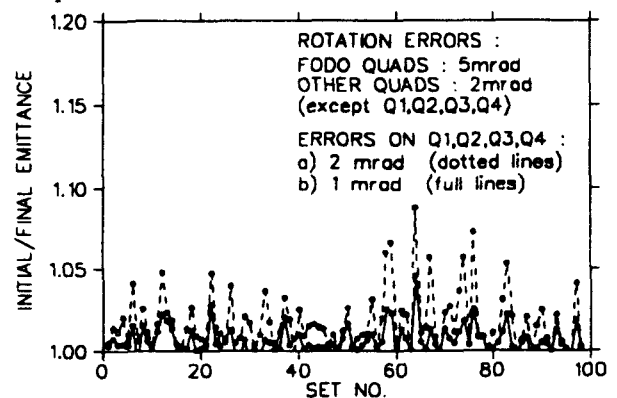


Figure 4: Emittance enlargement at the stripper due to rotation of the transfer line quadrupoles about the optic axis for 100 sets of random errors. Maximum magnitude of the errors are as specified on the figure.

VI. CONCLUSIONS

The linac-LEB transfer line for the SSC injector complex has a flexible design. It can handle almost four times the nominal emittance. Space charge effects can be optimized in a systematic way. Stringent LEB requirements allowing little emittance growth during injection are largely satisfied.

VII. ACKNOWLEDGEMENTS

We thank John McGill and Jerry Watson for several fruitful discussions and Deepak Raparia for supplying the results of the linac simulation studies.

VIII. REFERENCES

- [1] R. K. Bhandari and S. Penner, Proc. 1990 Linear Accelerator Conf., Sept. 10-14, 1990, Albuquerque, USA, (report no. LA-12004-C), p 411. Also report no. SSCL-339.
- [2] R. J. Macek, unpublished notes no. MP-5:86-28, May 5, 1986, Los Alamos National Lab., Los Alamos, USA.
- [3] S. Penner, "Injection -By-Stripping Loss Effects" unpublished notes, February 4, 1991.